Clinical Radiology 74 (2019) 918–925

Contents lists available at ScienceDirect

Clinical Radiology

journal homepage: www.clinicalradiologyonline.net

Whole solid tumour volume histogram analysis of the apparent diffusion coefficient for differentiating high-grade from low-grade serous ovarian carcinoma: correlation with Ki-67 proliferation status

H.M. Li [a,b,c,1], R. Zhang [d,1], W.Y. Gu [e], S.H. Zhao [f], N. Lu [g], G.F. Zhang [h], W.J. Peng [a,b,**], J.W. Qiang [c,*]

[a] Department of Radiology, Fudan University Shanghai Cancer Center, Shanghai 200032, China
[b] Department of Oncology, Shanghai Medical College, Fudan University, Shanghai 200032, China
[c] Department of Radiology, Jinshan Hospital, Fudan University, Shanghai 201508, China
[d] Department of Medical Imaging, Suzhou Institute of Biomedical Engineering and Technology, Chinese Academy of Sciences, Suzhou 215163, China
[e] Department of Pathology, Obstetrics & Gynecology Hospital, Fudan University, Shanghai 200011, China
[f] Department of Radiology, Xinhua Hospital, Shanghai Jiao Tong University, Shanghai 200092, China
[g] Department of Radiology, Huashan Hospital North, Fudan University, Shanghai 201907, China
[h] Department of Radiology, Obstetrics & Gynecology Hospital, Fudan University, Shanghai 200011, China

ARTICLE INFORMATION

Article history:
Received 10 December 2018
Accepted 24 July 2019

AIM: To investigate whether apparent diffusion coefficient (ADC) histogram parameters based on whole solid tumour volume could differentiate high-grade (HGSOC) from low-grade serous ovarian carcinoma (LGSOC) and to correlate those parameters with the Ki-67 proliferation index.

MATERIALS AND METHODS: One hundred and seven patients with HGSOCs and 19 patients with LGSOCs confirmed at surgery and histology who underwent conventional magnetic resonance imaging (MRI) and diffusion-weighted imaging (DWI) were analysed retrospectively. ADC histogram parameters (including the mean, standard deviation [SD], 10th, 25th, 50th, 75th, and 90th percentiles, kurtosis, and skewness) were obtained using the whole solid tumour volume region of interest (ROI). The Mann–Whitney *U* test, Pearson's chi-square test, Fisher's exact test, kappa test, Spearman's correlation, and receiver operating characteristic (ROC) curves were used for statistical analyses.

RESULTS: For ADC histogram parameters, the mean ($p<0.001$), SD ($p=0.003$), and all percentiles (10th, 25th, 50th, 75th, and 90th percentile; all $p<0.001$) were significantly lower in HGSOC than in LGSOC, and the area under the ROC curve (AUC) was 0.717–0.807. Skewness

* Guarantor and correspondent: J.W. Qiang, Department of Radiology, Jinshan Hospital, Fudan University, 1508 Longhang Road, Shanghai 201508, China. Tel.: +86 21 34189990; fax: +86 21 67226910.
** Guarantor and correspondent: W.J. Peng, Department of Radiology, Fudan University Shanghai Cancer Center, Department of Oncology, Shanghai Medical College, Fudan University, 270 Dongan Road, Shanghai 200032, China.
E-mail addresses: cjr.pengweijun@vip.163.com (W.J. Peng), dr.jinweiqiang@163.com (J.W. Qiang).
[1] These authors contribute equally to this manuscript.

https://doi.org/10.1016/j.crad.2019.07.019

was significantly higher in HGSOC than in LGSOC ($p<0.001$, AUC = 0.773); however, kurtosis was not significantly different between HGSOC and LGSOC ($p=0.140$). The 25th and 75th percentiles, SD and 10th percentile, and 75th percentile showed the highest sensitivity of 91.6%, specificity of 79.0%, and accuracy of 88.1%, respectively. All histogram parameters (except for kurtosis) were poorly correlated with the Ki-67 index ($|r| = 0.191–0.274$, $p<0.05$).

CONCLUSION: ADC histogram parameters based on whole solid tumour volume can be helpful for differentiating between HGSOC and LGSOC.

Introduction

High-grade serous ovarian carcinomas (HGSOCs) are the most common subtype of epithelial ovarian cancers (EOCs) and have high recurrence and mortality rates.[1] HGSOCs generally exhibit aggressive behaviour and most are diagnosed at advanced stages.[2] The primary treatments for patients with HGSOCs include comprehensive staging surgery, cytoreductive surgery, and platinum-based chemotherapy.[3] Despite the poor prognosis, most HGSOC patients show an initially high chemosensitivity.[4] In contrast, low-grade serous ovarian carcinomas (LGSOCs) are less common subtypes, accounting for 10% of serous EOCs.[5] LGSOCs typically occur in younger women and are usually slow-growing tumours with a relatively good prognosis, but similar to HGSOCs, most LGSOCs are high-stage tumours.[5,6] The treatment strategy of LGSOCs is comprehensive staging surgery followed by some postoperative management[3] and fertility-sparing surgery for some early-stage patients.[3] Neoadjuvant chemotherapy is not recommended because of the poor response.[7] Studies have suggested that hormonal maintenance therapy can improve the progression-free survival time.[8,9] HGSOCs and LGSOCs are two separate tumours with distinct origins, molecular abnormalities, biological behaviours, and treatment responses.[4,10] Accurate preoperative subtype diagnosis will be helpful for achieving a more effective subtype-specific treatment.[11]

Conventional magnetic resonance imaging (MRI) plays an important role in the differentiation of different types or subtypes of EOCs; however, some described conventional MRI morphological features are subjective and non-specific for diagnosis.[12] As a functional MRI technique, diffusion-weighted imaging (DWI) has been widely used in gynaecological imaging.[13] Although previous studies have evaluated the efficiency of simple mean values of apparent diffusion coefficients (ADCs) for differential diagnosis in ovarian tumours, the ADC values were measured on a single-slice or a “hot-spot” area.[14,15] Considering the large size and complexity of ovarian masses, mean ADC values could lead to some heterogeneous information being masked. In fact, histogram analysis based on whole solid tumour volume regions of interest (ROIs) could more accurately reflect the heterogeneity of ovarian carcinomas and provide additional information for clinical practice.[16] To date, only a few studies have focused on the application of histogram analysis in ovarian tumours.[17–19]

The Ki-67 antigen is the cell proliferation index that reflects the prognosis of malignant tumours. The ADC value can non-invasively assess tumour cellularity based on the Brownian motion of water molecules. Several studies have confirmed that the ADC value may be a reliable imaging marker reflecting Ki-67 expression.[15,20,21]

To the authors’ knowledge, however, there has been no study on the differentiation between HGSOCs and LGSOCs using ADC histogram analysis, and no study has evaluated the correlation between ADC histogram parameters and the Ki-67 index. Therefore, the purpose of the present study was to investigate the value of ADC histogram parameters derived from whole solid tumour volumes ROI in the differentiation of HGSOCs from LGSOCs and to correlate those parameters with the Ki-67 proliferation index.

Materials and methods

Patients

The institutional review board approved this retrospective study, and informed consent was waived. Between December 2010 and August 2017, a total of 147 consecutive patients were identified. Patients who had a history of chemotherapy before surgery ($n=9$), an intravoxel incoherent motion (IVIM) scan with b-values from 0 to 600 s/mm^2 ($n=5$), a poor image quality ($n=3$), no histopathological diagnosis ($n=2$), and a tumour with few solid components ($n=2$) were excluded. Finally, 126 patients with ovarian cancers (107 HGSOCs and 19 LGSOCs) confirmed by surgery and histology were included. The mean age was 53±9.2 years (range, 21–79 years). Histopathologically, borderline serous tumours (BOTs) with malignant transformation were observed in eight out of 19 cases of LGSOCs. Sixty-three patients (52 HGSOCs and 11 LGSOCs) had bilateral masses. To reduce the intra-individual effect, only the more complex lesion was included for further analysis. The tumours were staged according to the 2014 International Federation of Gynecology and Obstetrics (FIGO) staging system.[22]

MRI protocol

MRI examination was performed using a 1.5 T MRI machine (Avanto; Siemens, Erlangen, Germany) and phased-array abdominal coil. The conventional pelvic MRI

protocol consisted of the following sequences: axial and sagittal T2-weighted fat-suppressed fast-spin-echo (FSE), coronal T2-weighted FSE imaging, axial T1-weighted SE imaging, and axial pre- and post-contrast T1-weighted fat-suppressed 3D volumetric interpolated breath-hold examination (VIBE) imaging. For contrast-enhanced imaging, a dose of 0.2 mmol/kg gadopentetate dimeglumine (Magnevist; Bayer Schering, Berlin, Germany) was administered at a rate of 2–3 ml/s.

DWI was performed using a single-shot echo planar imaging (EPI) sequence. The parameters were as follows: 2,712–4,600 repetition time (TR), 83–94 ms/echo time (TE), 15–30 sections, 5 mm section thickness, 1.2 mm intersection gap, 280–350 mm field of view (FOV), 128×128 matrix, parallel imaging acceleration factor of 2, and 84–443 second acquisition time. The range and number of b-values exhibited some differences: b = 0 and 1000 s/mm^2; b = 0, 150, 500, 800, and 1,000 s/mm^2; b = 0, 50, 100, 150, 200, 400, 600, 800, 1,000, 1,500, and 2,000 s/mm^2; and b= 0, 500, 1,000, 1,500, 2,000, and 2,500 s/mm^2. ADC maps were generated using the images of two b factors (0 and 1000 s/mm^2).

Conventional image analysis

The conventional MRI images were analysed independently by two radiologists (with 9 [radiologist 1] and 10 years [radiologist 2] of experience in gynaecological imaging) who were blinded to the clinical data and histological diagnosis. The following MRI morphological features were analysed: (1) maximum diameter, measured on the axial images; (2) uni- or bilaterality; (3) mass configuration (mainly cystic, mixed cystic–solid, and solid tumours according to the criteria of less than one-third, one-to two-thirds and more than two-thirds solid components, respectively); and (4) enhancement (mild, moderate, and obvious by reference to the signal of the uterine junctional and outer myometrium). Any disagreements were solved in consensus, and the results were used for final analysis. To assess the interobserver agreement of MRI morphological features (mass configuration and enhancement), all 126 patients with 189 lesions were included.

ADC histogram analysis

For each patient, an ADC map was generated from the DWI with two b factors of 0 and 1000 s/mm^2 using in-house software (Siemens). DICOM data of ADC maps were imported into the MITK software (version 2013.12, http://mitk.org/wiki/MITK). The ROIs were manually delineated along the margin of the tumour solid component on each consecutive ADC map by radiologist 1. The solid components were determined by reference to T2-weighted, contrast-enhanced T1-weighted, and DWI images, and the cystic, necrosis, and haemorrhage areas were carefully excluded. All drawn ADC maps with ROIs were saved in the NRRD format. Thereafter, a pixel-by-pixel analysis was performed using pyradiomics software (http://pyradiomics.readthedocs.io/en/latest/index.html), which could automatically obtain the histogram parameters of ADC for whole solid tumour volume ROI, including the mean, standard deviation (SD), 10th, 25th, 50th, 75th, and 90th percentiles, kurtosis, and skewness.

Histopathological analysis

Ki-67 analysis was performed retrospectively by a gynaecological pathologist (with 12 years of experience) who was blinded to all MRI and clinicopathological data. Ki-67 expression was determined using the percentage of positively stained cells from 1,000 tumour cells (×400), and scoring was analysed in areas with the most positive nuclei ("hot-spot") within each tumour. The Ki-67 index was classified as a high-proliferation and low-proliferation group according to a cut-off value of 20%.[15]

Statistical analysis

All continuous variables were assessed for normality using a one-sample Kolmogorov–Smirnov test, and the data are expressed as the mean±standard deviation or median (interquartile range [IQR], 25th and 75th percentile). The differences between HGSOCs and LGSOCs for continuous and categorical variables were compared using the Mann–Whitney *U*-test, Pearson's chi-square test, and Fisher's exact test. The kappa test was used to evaluate the interobserver agreement of two categorical variables (mass configuration and enhancement). A Kappa coefficient of 0.81–1.00 indicated excellent agreement; 0.61–0.80 indicated good agreement; 0.41–0.60 indicated moderate agreement; 0.21–0.40 indicated fair agreement; and 0–0.20 indicated poor agreement. The association between ADC histogram parameters and the Ki-67 index was assessed using Spearman's correlation. The diagnostic performance of ADC histogram parameters was evaluated using ROCs, and the AUC of each parameter was used to assess the discriminative power. The sensitivity, specificity, and accuracy were calculated based on the cut-off value. The differences in AUC for histogram parameters were compared using the DeLong method.[23] SPSS 23.0 (IBM, Armonk, NY, USA) and Medcalc 7.4.2.0 (Mariakerke, Belgium) were used for the statistical analysis. A p-value of <0.05 was deemed statistically significant.

Results

Clinical and MRI morphological features

The mean age of 107 patients with HGSOCs was 54.6±7.9 years (range, 35–79 years), which was significantly greater than that of 19 patients with LGSOCs (44.1±10.8 years; range, 21–58 years; $p<0.001$). Sixty-six patients (66/107, 61.7%) with HGSOCs were stage III, followed by stage II (17/107, 15.9%), stage I (15/107, 14.0%), and stage IV (9/107, 8.4%); the percentages were 47.4% (9/19), 26.3% (5/19), 21.1% (4/19), and 5.3% (1/19) for patients with LGSOCs, respectively. No significant difference in FIGO stage was found between HGSOCs and LGSOCs ($p=0.488$).

Table 1 shows the comparisons of MRI morphological features between HGSOCs and LGSOCs. HGSOCs displayed a mild, moderate, and obvious enhancement in 32.7%, 35.5% and 31.8% of cases, while LGSOCs mainly showed an obvious enhancement (12/19, 63.3%; p=0.032). There were no significant differences between HGSOCs and LGSOCs in tumour maximum diameter, bilaterality, and configuration (p=0.433, 0.455, and 0.352, respectively). The Kappa test showed excellent and good interobserver agreement for the evaluation of mass configuration and enhancement (with Kappa coefficients of 0.852 and 0.710, respectively).

ADC histogram parameters and ROC analysis

Comparisons of ADC histogram parameters between HGSOCs and LGSOCs are presented in Table 2. The mean value, SD, and percentiles (10th, 25th, 50th, 75th, and 90th percentile) of HGSOCs were significantly lower than those of LGSOCs (all p<0.001, except p=0.003 for SD). Conversely, HGSOCs had significantly higher skewness compared with LGSOCs (p<0.001). The kurtosis was not significantly different between HGSOC and LGSOC (p=0.140). Representative cases of HGSOCs and LGSOCs for histogram analysis of ADC are shown in Figs 1–3.

The diagnostic performances of ADC histogram parameters are summarised in Table 3. ROC curve analyses showed that the 25th and 75th percentiles of ADC values had the highest sensitivity of 91.59%, the 75th percentile had the highest accuracy of 88.10%, and the SD and 10th percentile showed the highest specificity of 78.95%; however, there were no significant differences in AUC between each of the eight histogram parameters.

Table 1
Conventional MRI morphological features of high-grade (HGSOC) from low-grade serous ovarian carcinoma (LGSOC).

Features	HGSOCs (n=107)	LGSOCs (n=19)	p-Value
Maximum diameter (cm)	8.7±3.4	9.2±3.0	0.433
Bilaterality	52/107 (48.6%)	11/19 (57.9%)	0.455
Configuration			0.352
Predominantly cystic	29/107 (27.1%)	7/19 (36.8%)	
Mixed cystic-solid	25/107 (23.4%)	6/19 (31.6%)	
Solid	53/107 (49.5%)	6/19 (31.6%)	
Enhancement			0.032
Mild	35/107 (32.7%)	3/19 (15.8%)	
Moderate	38/107 (35.5%)	4/19 (21.1%)	
Obvious	34/107 (31.8%)	12/19 (63.2%)	

Table 2
Comparisons of apparent diffusion coefficient histogram parameters between high-grade (HGSOC) from low-grade serous ovarian carcinoma (LGSOC).

Parameters	HGSOCs (n=107)	LGSOCs (n=19)	p-Value
Mean	0.986 [0.872,1.155]	1.425 [1.104,1.583]	<0.001
Standard deviation	0.207 [0.176,0.247]	0.248 [0.229,0.316]	0.003
10th percentile	0.748 [0.665,0.896]	1.042 [0.892,1.281]	<0.001
25th percentile	0.840 [0.737,1.009]	1.218 [0.963,1.417]	<0.001
Median	0.956 [0.857,1.139]	1.428 [1.075,1.577]	<0.001
75th percentile	1.103 [0.968,1.299]	1.595 [1.305,1.739]	<0.001
90th percentile	1.262 [1.131,1.503]	1.746 [1.387,1.990]	<0.001
Kurtosis	3.731 [3.250,5.141]	3.523 [2.907,4.042]	0.140
Skewness	0.754 [0.465,1.099]	0.127 [−0.217,0.484]	<0.001

Data are median [interquartile range] ($\times 10^{-3}$mm^2/s).

Correlation between the Ki-67 index and ADC histogram parameters

The Ki-67 proliferation index was available for 99 patients with HGSOCs and 17 patients with LGSOCs. Eighty-six patients with HGSOCs (86/99, 86.9%) showed high proliferation based on Ki-67, while 12 patients with LGSOCs (12/17, 70.6%) showed low proliferation. The median Ki-67 index was 40% (30%, 70%) in HGSOCs and 10% (5%, 20%) in LGSOCs (p<0.001). The mean, SD, and the 10th, 25th, 50th, 75th, and 95th percentiles were negatively correlated with the Ki-67 index (r=−0.260, −0.191, −0.248, −0.264, −0.274, −0.265, and −0.255, respectively), while skewness was positively correlated with the Ki-67 index (r=0.250).

Discussion

The present preliminary study showed that ADC histogram parameters based on whole solid tumour volume analysis were useful for differentiating between HGSOCs and LGSOCs. The lower histogram metrics of the mean, SD, percentiles, and higher skewness represent HGSOC, and vice versa for LGSOC; however, no MRI morphological features except enhancement were significantly different between HGSOCs and LGSOCs. HGSOCs had a significantly higher Ki-67 index than LGSOCs; however, only poor correlations were found between ADC histogram parameters and the Ki-67 index.

Tumour heterogeneity is an important characteristic of malignant tumours.[24] Histogram analysis can allow the visualisation of heterogeneous information and provide quantitative image markers for evaluating tumours. Ovarian carcinomas are more likely to exhibit cystic and necrotic degenerations, which can lead to greater heterogeneity of water diffusion. The quantitative parameters based on a single-section ROI could not comprehensively and accurately reflect the biological characteristics of the tumour, whereas whole solid tumour volume histogram analysis could calculate the ADC values of each voxel and objectively reflect the heterogeneity of the entire tumour; thus, the results might be more reliable and repeatable for clinical application.[16] Previous studies in ADC histogram analysis have mainly focused on the tumour differential diagnosis, histological subtype, differentiation or grade, therapeutic response, and prediction of prognosis.[25–29]

The present results demonstrated that all ADC histogram parameters except kurtosis were significantly different between HGSOCs and LGSOCs. The mean and percentile values of ADC were significantly lower in HGSOCs than in LGSOCs, which was consistent with previous studies on the differentiation of EOC types and mucinous breast carcinoma subtype.[18,30] The pathological basis of these findings was that HGSOCs have a larger cell density and ratio of nucleus to cytoplasm, which limited water molecule diffusion in extra- and intracellular spaces. Kang *et al.*[31] found that the

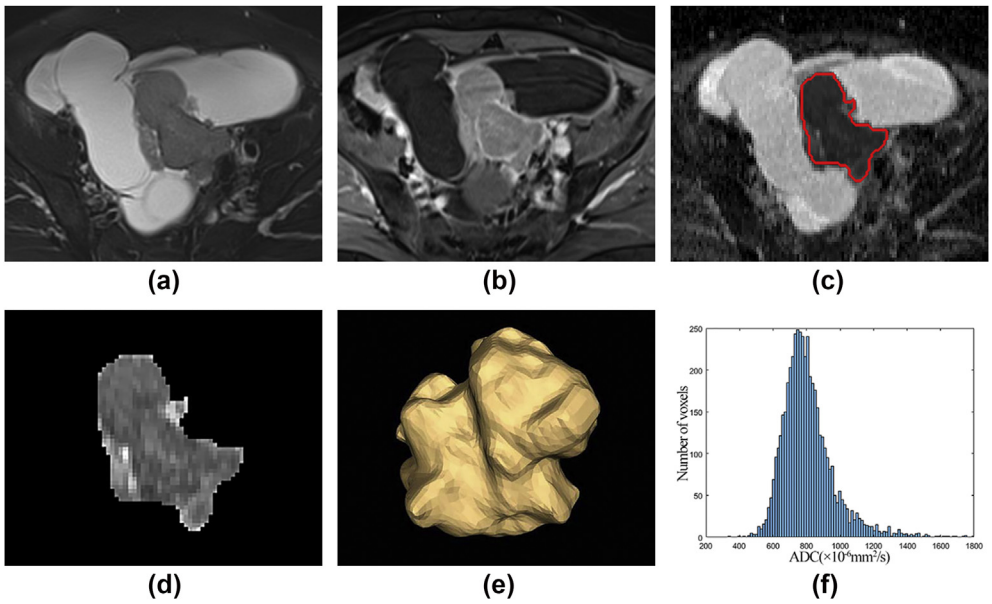

Figure 1 A 53-year-old woman with HGSOC in the right ovary. (a) Axial T2-weighted image shows a mixed cystic-solid mass. (b) Axial contrast-enhanced T1-weighted image shows a mild enhancement in the solid component. The red ROI was manually drawn along the margin of the solid component on the ADC map (c). The segmented solid region (d) and three-dimensional map of the tumour (e) are obtained. (f) The ADC histogram more frequently shows low ADC values.

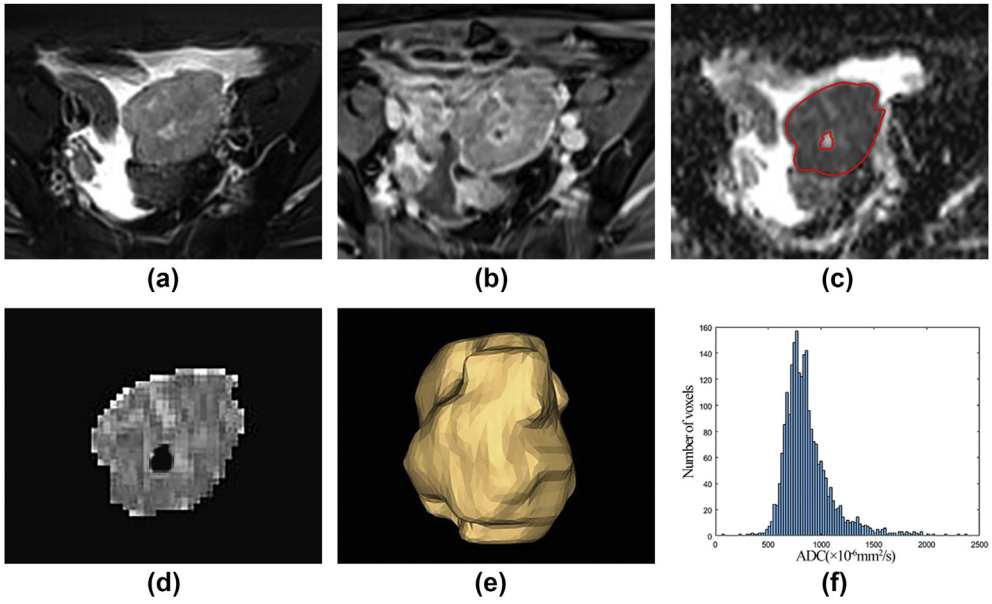

Figure 2 A 59-year-old woman with HGSOC in bilateral ovaries. An axial T2-weighted image (a) and a contrast-enhanced T1-weighted image (b) show a larger, mildly enhanced solid mass in the left ovary. The tumour shows a notably low intensity on the ADC map (c). The segmented solid region (d) and three-dimensional map of the tumour (e) are shown. The graph shows the corresponding ADC histogram (f).

5th percentile of the ADC histogram based on a high b-value of 3,000 s/mm^2 was the best parameter for differentiating high-from low-grade gliomas. Mimura *et al.*[19] found that the 10th percentile of ADC values had the highest AUC for differentiating borderline from malignant ovarian tumours. Studies by Takahashi *et al.*[32] and Chandarana *et al.*[33] showed that the 75th percentile of ADC value and the third quartile enhancement were the two most accurate parameters for differentiating uterine carcinosarcomas from endometrial carcinomas and renal clear cell cancer from papillary cancer, respectively. These studies demonstrated the additional value of histogram parameters for the differentiation of the subtypes of malignant tumours. In the present study, although no significant difference was observed between any two AUCs of the mean and percentiles, ROC curves showed that percentiles appeared to have complementary

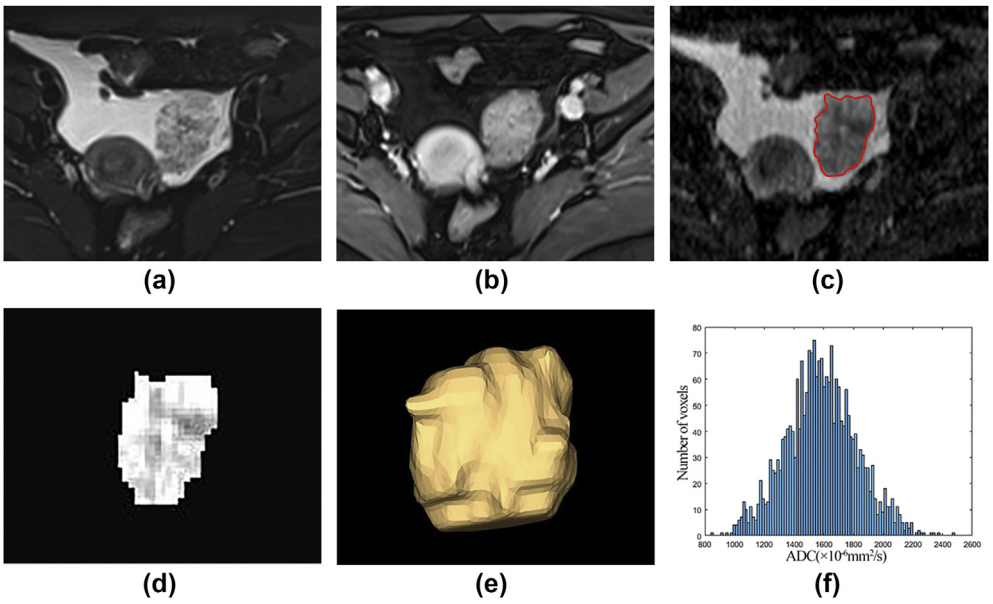

Figure 3 A 57-year-old woman with LGSOC in the left ovary. An axial T2-weighted image (a) and a contrast-enhanced T1-weighted image (b) show a markedly enhanced solid mass. The tumour shows moderate intensity on the ADC map (c). The segmented solid region (d) and three-dimensional map of the tumour (e) are shown. (f) The ADC histogram more frequently shows high ADC values.

Table 3
Diagnostic performances of apparent diffusion coefficient histogram parameters for differentiating high-grade from low-grade serous ovarian carcinoma.

Parameters	AUC	95% CI	Threshold	Sensitivity	Specificity	Accuracy
Mean	0.798	0.717, 0.862	≤1.289	88.79%	68.42%	85.71%
SD	0.717	0.630, 0.794	≤0.227	65.42%	78.95%	67.46%
10th percentile	0.775	0.692, 0.845	≤0.876	74.77%	78.95%	75.40%
25th percentile	0.801	0.720, 0.867	≤1.177	91.59%	63.16%	87.30%
Median	0.807	0.727, 0.872	≤1.306	89.72%	68.42%	86.51%
75th percentile	0.803	0.722, 0.868	≤1.507	91.59%	68.42%	88.10%
90th percentile	0.786	0.704, 0.854	≤1.648	89.72%	68.42%	86.51%
Skewness	0.773	0.690, 0.843	≥0.375	79.44%	73.68%	78.57%

AUC, area under the curve; CI, confidence interval; SD, standard deviation.

advantages in differentiating HGSOCs from LGSOCs and that the 75th percentile provided the highest diagnostic accuracy.

The SD represents the dispersion of the ADC histogram. The present results demonstrate that the SD value was significantly higher in LGSOCs than in HGSOCs. Increasing with the SD value, the ADC histogram distribution becomes more disperse and thus has larger heterogeneity. A pathological study has confirmed that serous borderline tumours are the precursor lesions of LGSOCs.[34] The study by Okoye *et al.*[35] showed that 28 out of 33 patients with LGSOC had borderline components, and 15 LGSOCs were mainly composed of borderline components. The mean ADC values of borderline ovarian tumours were significantly higher than those of epithelial ovarian carcinomas in a study by Zhao *et al.*[14] Therefore, the higher SD of LGSOCs might be due to the concurrent borderline components.

Skewness is a statistical measure of the asymmetric distribution of the ADC value. Previous studies have shown that the skewness of ADC was useful for predicting and monitoring the response to treatment for advanced rectal carcinoma and ovarian carcinoma.[17,28] In the present study, skewness was significantly higher in HGSOCs than in LGSOCs. This finding indicated that there were more voxels of the ADC values below the mean in HGSOCs than in LGSOCs. In particular, the 25 percentile of skewness showed a negatively skewed distribution in LGSOCs, which contained more values on the right side of the mean.

Kurtosis reflects the peakedness of ADC histogram distribution. Kurtosis can predict the aggressiveness of pancreatic neuroendocrine tumours.[36] Kurtosis is also a reliable biomarker for predicting treatment failure in head and neck squamous cell carcinoma[37]; however, no significant difference in kurtosis between HGSOCs and LGSOCs was observed in the present study.

Several previous studies have demonstrated the value of quantitative DWI parameters for predicting the proliferation status based on Ki-67 in different organs[15,20,21]; however, a poor correlation was found between ADC histogram parameters and the Ki-67 index in the present study, which was consistent with the study by Aydin *et al.*[38] on invasive ductal carcinoma. A possible explanation was that the proliferation index was analysed in the densest areas of tumour cells (so-called “hot spots”), whereas the ADC

histogram parameters were measured based on the entire solid components and the marked intratumoural heterogeneity. Therefore, further studies are needed to determine whether the ADC histogram parameters can non-invasively reflect the Ki-67 proliferation status.

The present study had several limitations. First, because of the nature of the retrospective study, population selection biases were inevitable. Second, the range and number of b-values are different, which might affect the accuracy of ADC histogram parameter measurements. Third, the present preliminary results were obtained based on a single centre with a small sample of LGSOCs due to the low incidence. Therefore, the reliability of the findings needs to be verified by large-scale and multicentre prospective studies. Fourth, despite the advantages of ADC histogram analysis, the intra- and interobserver repeatability of ADC measurements were not evaluated. Finally, ADC value measurement based on manually drawing ROIs might be accurate, but the analysis was time-consuming and inefficient for clinical application; however, the novel semi-automatic or automatic image segmentation methods could not only eliminate the influence of artificial factors, but also result in highly repeatable or time-efficient results.

In conclusion, the present study showed that ADC histogram parameters based on whole solid tumour volume ROIs were useful for differentiating between HGSOCs and LGSOCs.

Declaration of interest

The authors declare no conflict of interest.

Acknowledgements

This study was funded by the National Natural Science Foundations of China (grant nos. 81471628, 81501439, and 81701686) and the Imaging Foundation of Fudan University Shanghai Cancer Center (grant no. YX201803).

References

1. Labidi-Galy SI, Papp E, Hallberg D, *et al*. High grade serous ovarian carcinomas originate in the fallopian tube. *Nat Commun* 2017;**8**(1):1093.
2. Bowtell DD, Böhm S, Ahmed AA, *et al*. Rethinking ovarian cancer II: reducing mortality from high-grade serous ovarian cancer. *Nat Rev Cancer* 2015;**15**(11):668–79.
3. National Comprehensive Cancer Network. NCCN clinical practice guidelines in oncology: ovarian cancer including fallopian tube cancer and primary peritoneal cancer, version 2. Available at: https://www.nccn.org/professionals/physician_gls/default.aspx#nmsc; March 9, 2018.
4. Gurung A, Hung T, Morin J, *et al*. Molecular abnormalities in ovarian carcinoma: clinical, morphological and therapeutic correlates. *Histopathology* 2013;**62**(1):59–70.
5. Kaldawy A, Segev Y, Lavie O, *et al*. Low-grade serous ovarian cancer: a review. *Gynecol Oncol* 2016;**143**(2):433–8.
6. Chen M, Jin Y, Bi Y, *et al*. A survival analysis comparing women with ovarian low-grade serous carcinoma to those with high-grade histology. *Onco Targets Ther* 2014;**7**:1891–9.
7. Gourley C, Farley J, Provencher DM, *et al*. Gynecologic Cancer InterGroup (GCIG) consensus review for ovarian and primary peritoneal low-grade serous carcinomas. *Int J Gynecol Cancer* 2014;**24**(Suppl. 3):S9–13.
8. Fader AN, Bergstrom J, Jernigan A, *et al*. Primary ctyoreductive surgery and adjuvant hormonal monotherapy in women with advanced low-grade serous ovarian carcinoma: reducing overtreatment without compromising survival? *Gynecol Oncol* 2017;**147**(1):85–91.
9. Köbel M, Kalloger SE, Boyd N, *et al*. Ovarian carcinoma subtypes are different diseases: implications for biomarker studies. *PLoS Med* 2008;**5**(12):e232.
10. Gershenson DM, Bodurka DC, Coleman RL, *et al*. Hormonal maintenance therapy for women with low-grade serous cancer of the ovary or peritoneum. *J Clin Oncol* 2017;**35**(10):1103–11.
11. Despierre E, Yesilyurt BT, Lambrechts S, *et al*. Epithelial ovarian cancer: rationale for changing the one-fits-all standard treatment regimen to subtype-specific treatment. *Int J Gynecol Cancer* 2014;**24**(3):468–77.
12. Lalwani N, Prasad SR, Vikram R, *et al*. Histologic, molecular, and cytogenetic features of ovarian cancers: implications for diagnosis and treatment. *RadioGraphics* 2011;**31**(3):625–46.
13. Pi S, Cao R, Qiang JW, *et al*. Utility of DWI with quantitative ADC values in ovarian tumours: a meta-analysis of diagnostic test performance. *Acta Radiol* 2018;**59**(11):1386–94.
14. Zhao SH, Qiang JW, Zhang GF, *et al*. Diffusion-weighted MR imaging for differentiating borderline from malignant epithelial tumours of the ovary: pathological correlation. *Eur Radiol* 2014;**24**(9):2292–9.
15. Li HM, Zhao SH, Qiang JW, *et al*. Diffusion kurtosis imaging for differentiating borderline from malignant epithelial ovarian tumours: a correlation with Ki-67 expression. *J Magn Reson Imaging* 2017;**46**(5):1499–506.
16. Just N. Improving tumour heterogeneity MRI assessment with histogram. *Br J Cancer* 2014;**111**(12):2205–13.
17. Kyriazi S, Collins DJ, Messiou C, *et al*. Metastatic ovarian and primary peritoneal cancer: assessing chemotherapy response with diffusion-weighted MR imaging- value of histogram analysis of apparent diffusion coefficients. *Radiology* 2011;**261**(1):182–92.
18. Wang F, Wang Y, Zhou Y, *et al*. Comparison between types I and II epithelial ovarian cancer using histogram analysis of monoexponential, biexponential, and stretched- exponential diffusion models. *J Magn Reson Imaging* 2017;**46**(6):1797–809.
19. Mimura R, Kato F, Tha KK, *et al*. Comparison between borderline ovarian tumours and carcinomas using semi-automated histogram analysis of diffusion-weighted imaging: focusing on solid components. *Jpn J Radiol* 2016;**34**(3):229–37.
20. Xiao ZB, Zhong Y, Tang Z, *et al*. Standard diffusion-weighted, diffusion kurtosis and intravoxel incoherent motion MR imaging of sinonasal malignancies: correlations with Ki-67 proliferation status. *Eur Radiol* 2018;**28**(7):2923–33.
21. Hu XX, Yang ZX, Liang HY, *et al*. Whole-tumour MRI histogram analyses of hepatocellular carcinoma: correlations with Ki-67 labeling index. *J Magn Reson Imaging* 2017;**46**(2):383–92.
22. Mutch DG, Prat J. 2014 FIGO staging for ovarian, fallopian tube and peritoneal cancer. *Gynecol Oncol* 2014;**133**(3):401–4.
23. DeLong ER, DeLong DM, Clarke-Pearson DL. Comparing the area under two or more correlated receiver operating characteristic curves: a nonparametric approach. *Biometrics* 1988;**44**(3):837–45.
24. Gerlinger M, Rowan AJ, Horswell S, *et al*. Intratumour heterogeneity and branched evolution revealed by multiregion sequencing. *N Engl J Med* 2012;**336**(10):883–92.
25. Gerges L, Popiolek D, Rosenkrantz AB. Explorative investigation of whole-lesion histogram MRI metrics for differentiating uterine leiomyomas and leiomyosarcoma. *AJR Am J Roentgenol* 2018;**210**(5):1172–7.
26. Li A, Xing W, Li H, *et al*. Subtype differentiation of small (≤4 cm) solid renal mass using volumetric histogram analysis of DWI at 3-T MRI. *AJR Am J Roentgenol* 2018;**211**(3):614–23.
27. Zhang Y, Chen J, Liu S, *et al*. Assessment of histological differentiation in gastric cancers using whole-volume histogram analysis of apparent diffusion coefficient maps. *J Magn Reson Imaging* 2017;**45**(2):440–9.
28. Enkhbaatar NE, Inoue S, Yamamuro H, *et al*. MR imaging with apparent diffusion coefficient histogram analysis: evaluation of locally advanced rectal cancer after chemotherapy and radiation therapy. *Radiology* 2018;**288**(1):129–37.
29. Kondo M, Uchiyama Y. Apparent diffusion coefficient histogram analysis for prediction of prognosis in glioblastoma. *J Neuroradiol* 2018;**45**(4):236–41.
30. Guo Y, Kong QC, Zhu YQ, *et al*. Whole-lesion histogram analysis of the apparent diffusion coefficient: evaluation of the correlation with

subtypes of mucinous breast carcinoma. *J Magn Reson Imaging* 2018; **47**(2):391–400.
31. Kang Y, Choi SH, Kim YJ, *et al*. Gliomas: histogram analysis of apparent diffusion coefficient maps with standard- or high-b-value diffusion-weighted MR imaging- correlation with tumour grade. *Radiology* 2011;**261**(3):882–90.
32. Takahashi M, Kozawa E, Tanisaka M, *et al*. Utility of histogram analysis of apparent diffusion coefficient maps obtained using 3.0T MRI for distinguishing uterine carcinosarcoma from endometrial carcinoma. *J Magn Reson Imaing* 2016;**43**(6):1301–7.
33. Chandarana H, Rosenkrantz AB, Mussi TC, *et al*. Histogram analysis of whole-lesion enhancement in differentiating clear cell from papillary subtype of renal cell cancer. *Radiology* 2012;**265**(3):790–8.
34. Lim D, Oliva E. Precursors and pathogenesis of ovarian carcinoma. *Pathology* 2013;**45**(3):229–42.
35. Okoye E, Euscher ED, Malpica A. Ovarian low-grade serous carcinoma: a clinicopathologic study of 33 cases with primary surgery performed at a single institution. *Am J Surg Pathol* 2016;**40**(5):627–35.
36. De Robertis R, Maris B, Cardobi N, *et al*. Can histogram analysis of MR images predict aggressiveness in pancreatic neuroendocrine tumours? *Eur Radiol* 2018;**28**(6):2582–91.
37. King AD, Chow KK, Yu KH, *et al*. Head and neck squamous cell carcinoma: diagnostic performance of diffusion-weighted MR imaging for the prediction of treatment response. *Radiology* 2013;**266**(2):531–8.
38. Aydin H, Guner B, Esen Bostanci I, *et al*. Is there any relationship between ADC values of diffusion-weighted imaging and the histopathological prognostic factors of invasive ductal carcinoma? *Br J Radiol* 2018;**91**(1084):2017070.